Cellulose (2016) 23:379–390
DOI 10.1007/s10570-015-0812-y

ORIGINAL PAPER

Individualization of microfibrillated celluloses from oil palm empty fruit bunch: comparative studies between acid hydrolysis and ammonium persulfate oxidation

Kar Yin Goh · Yern Chee Ching · Cheng Hock Chuah · Luqman Chuah Abdullah · Nai-Shang Liou

Received: 10 June 2015 / Accepted: 2 November 2015 / Published online: 12 November 2015

Abstract In the present study, the feasibility and the practicability of two different approaches to the individualization of microfibrillated celluloses (MFCs) from oil palm empty fruit bunches were evaluated. Some properties of MFCs prepared by ammonium persulfate (APS) oxidation were investigated and compared with those extracted using sulfuric acid hydrolysis. Fourier transform infrared observation demonstrated that almost all the hemicelluloses and lignin were effectively removed after the sulfuric acid hydrolysis, which was substantiated by the disappearance of the characteristic peaks of these two noncellulosic components at 1735 and 1508 cm^{-1}, respectively. However, a peak at 1735 cm^{-1} was observed in the spectrum of APS-oxidized MFCs because the products prepared by this treatment are stabilized by carboxyl groups instead of sulfate half-ester groups, which introduced by sulfuric acid. Furthermore, X-ray diffractograms of MFCs revealed the decrease in crystallinity after sulfuric acid hydrolysis but remained similar after APS oxidation. Thermogravimetric analysis was employed to determine the thermal stability of the treated fibers. In addition, the morphologies and diameters of MFCs were determined by field-emission scanning electron microscopy. MFCs formed by these two different techniques exhibited long and network-like fibrils with widths ranging from 8 to 40 nm. UV-Vis spectroscopy was used to monitor the optical transmittance of the nanocellulose suspensions.

Keywords Oil palm empty fruit bunch · Microfibrillated celluloses · Ammonium persulfate oxidation · Carboxyl groups · Sulfuric acid hydrolysis · Sulfate half-ester groups

K. Y. Goh · Y. C. Ching (✉)
Department of Mechanical Engineering, Faculty of Engineering, University of Malaya, 50603 Kuala Lumpur, Malaysia
e-mail: chingyc@um.edu.my

K. Y. Goh · C. H. Chuah
Department of Chemistry, Faculty of Science, University of Malaya, 50603 Kuala Lumpur, Malaysia

L. C. Abdullah
Department of Chemical Engineering, Faculty of Engineering, University Putra Malaysia, 43400 Serdang, Malaysia

N.-S. Liou
Department of Mechanical Engineering, Southern Taiwan University of Science and Technology, Yungkang Dist., Tainan City 710, Taiwan, ROC

Abbreviations

APS	Ammonium persulfate
CNCs	Cellulose nanocrystals
CrI	Crystallinity index
FESEM	Field-emission scanning electron microscopy
FTIR	Fourier transform infrared
HCl	Hydrochloric acid

HNO_3	Nitric acid
H_2O	Water molecule
H_2O_2	Hydrogen peroxide
HSO_4^-	Hydrogen sulfate ion
H_2SO_4	Sulfuric acid
KBr	Potassium bromide
MFC	Microfibrillated cellulose
$NaClO_2$	Sodium chlorite
NaOH	Sodium hydroxide
NCCs	Nanocrystalline celluloses
OPEFB	Oil palm empty fruit bunch
$SO_4^{\cdot-}$	Sulfate radical anion
$S_2O_8^{2-}$	Peroxydisulfate ion
TGA	Thermogravimetric analysis
UV-Vis	Ultraviolet-visible
XRD	X-ray diffraction

Introduction

Natural fibers have garnered considerable attention in the industry and research areas because of their distinctive properties, which include excellent mechanical strength, biodegradability, renewability, low density as well as ease of surface modification (Azizi Samir et al. 2005; Nurfatimah et al. 2014; Ashiqur et al. 2015; Ershad et al. 2015; Yong et al. 2015a; Tan et al. 2015). Cellulose is an inexhaustible source of biopolymer; thus, it is anticipated to be cost effective because of its high availability (Cherian et al. 2011). Cellulose can be processed in nanoscale dimensions with a plethora of potential applications including as a drug carrier (Jackson et al. 2011), paper additive (Sehaqui et al. 2011) and enzyme immobilizer (Mahmoud et al. 2009). Owing to its remarkable mechanical properties, cellulose has emerged as a prominent candidate to replace synthetic reinforcing fillers in bio-nanocomposites, polymetric matrixes and biodegradable composites (Cherian et al. 2011; Tan et al. 2015). The utilization of these undesirable wastes is a clear advantage in terms of environmental impact (El-Saied et al. 2012).

Acid hydrolysis (Lu and Hsieh 2012; Ching and Ng 2014; Ching et al.2015), mechanical disintegration (Li et al. 2012), TEMPO-mediated oxidation (Tanaka et al. 2012) and enzyme-assisted hydrolysis (Janardhnan and Sain 2007) are some of the promising approaches employed to isolate celluloses from numerous sources of lignocellulosic biomass materials. Among these techniques, sulfuric acid hydrolysis is recognized to be the most common method to selectively remove the amorphous regions of cellulose, producing highly crystalline cellulose nanoparticles known as cellulose nanocrystals (CNCs) or nanocrystalline celluloses (NCCs) (Abraham et al. 2011). Generally, nanocelluloses have diameters of less than 100 nm and are tens to hundreds of nanometers long (Lam et al. 2013). Thus, they have a large surface-to-volume ratio (Huang et al. 2003). Manipulating several parameters such as the temperature, reaction time and acid concentration allows some variations in the dimensions of the final derived nanocelluloses (Fatah et al. 2014).

Nevertheless, sulfuric acid hydrolysis displays some drawbacks in terms of productivity and thermal stability (Qua et al. 2011; Ng et al. 2014). According to Qua et al. (2011), small quantities of nanofibers that are approximately 30 % on a weight basis will be produced as the final yield using this method, which causes difficulty in scaling up the production. In addition, the sulfate half ester groups incorporated into the nanofibers after sulfuric acid hydrolysis will potentially have a detrimental effect on the thermal properties of the CNCs produced (Roman and Winter 2004). Furthermore, removal of the noncellulosic components such as hemicelluloses, lignin and waxes is a prerequisite prior to the isolation of CNCs (Leung et al. 2011). Hence, multiple chemical procedures are involved to eliminate the noncellulosic constituents before the acid hydrolysis. With this technique, tedious and time-consuming preparation steps are required to obtain nanocelluloses.

However, all these difficulties can be avoided because of the exciting discovery of the isolation of carboxylated nanocelluloses via an effective and a green procedure using ammonium persulfate (APS) (Leung et al. 2011; Castro-Guerrero and Gray 2014; Lam et al. 2013). Ammonium persulfate is a strong oxidant that performs versatile functions to generate nanocelluloses in a one-step procedure without any pretreatment. Removal of hemicellulose and lignin as well as the bleaching of fiber can be easily attained in a simple method. The in situ exclusion of these noncellulosic components and amorphous regions can be explained by the postulated mechanism whereby $SO_4^{\cdot-}$, HSO_4^- and hydrogen peroxide are formed during the course of nanocellulose synthesis by APS (Leung et al. 2011). Formation of free radicals will be

induced when heat is applied to the solution containing persulfate ($S_2O_8^{2-} + \text{heat} \rightarrow 2SO_4^{\cdot-}$). Under acidic conditions (pH 1.0), hydrogen peroxide is also formed ($S_2O_8^{2-} + 2H_2O \rightarrow 2HSO_4^- + H_2O_2$) (Hsu et al. 2002). Both free radicals $SO_4^{\cdot-}$ and H_2O_2 are capable of penetrating the amorphous domains as well as performing the decolorization of the materials (Leung et al. 2011). In contrast to sulfuric acid hydrolysis, this method generates some carboxyl groups on the nanocellulose surface. This method is amenable to large-scale nanocellulose production and is applicable to a variety of cellulosic biomasses (Leung et al. 2011).

In some particular applications, especially tissue-engineering scaffolds, fine and long nanofibers are indispensable as they are required to emulate the native extracellular matrix (ECM) for nutrient transport as well as cell attachment (Coburn et al. 2011). Microfibrillated cellulose (MFC) is another type of nanofiber that has elicited much interest, having similar features as cellulose nanocrystals but with a higher aspect ratio (L/d) (Lin et al. 2012). MFCs exhibit long and network-like structures (Lin et al. 2012) with widths ranging from 30 to 100 nm and are several micrometers in lengths (Fatah et al. 2014). MFC production is normally achieved by means of mechanical disintegrations such as homogenization (Zhao et al. 2013), microfluidization (Ferrer et al. 2012) and ultrasonication (Chen et al. 2011a, b). In this work, we attempted to treat oil palm empty fruit bunches (OPEFBs) individually by sulfuric acid hydrolysis or APS oxidation to extract MFCs as well as examine some of the properties of the resultant MFCs.

Experimental

Materials

The OPEFB fibers were provided by Sabutek Sdn. Bhd., Malaysia, and were used as the starting material. Sodium hydroxide (NaOH) pellets, glacial acetic acid, 65 % nitric acid (HNO_3), 95–97 % sulfuric acid (H_2SO_4) and ammonium persulfate (APS) were purchased from Friendemann Schmidt Chemicals. Sodium chlorite ($NaClO_2$) (80 %) and absolute ethanol were supplied by Sigma-Aldrich and Kollin Chemicals, respectively.

Extraction of microfibrillated celluloses by acid hydrolysis

OPEFB fibers were passed through a 45-μm sieve. First, the resins, waxes and oil components of OPEFBs were removed by Soxhlet extraction using 250 ml 70 % (v/v) ethanol as solvent for 24 h. The extractive-free fibers were washed with boiled water. Next, 6 wt% NaOH solution was prepared and added to the extracted samples for 4 h at 30 °C, which resulted in swelling of the fiber and subsequent increases in the moisture absorption (Abraham et al. 2011; Tan et al. 2014). For the removal of hemicelluloses, swollen fibers were treated with a higher concentration of NaOH solution (17.5 wt% of NaOH). This was conducted at 80 °C for 4 h under constant mechanical stirring. After the treatment, the fibers were subjected to centrifugation and washed with distilled water to remove the alkali-soluble components as well neutralize the fibers. A subsequent bleaching process was carried out by adding equal parts of acetate buffer (solution of 2.7 g NaOH and 7.5 ml glacial acetic acid in 100 ml distilled water) and 1.7 wt% aqueous chlorite to the treated fibers for 4 h at 80 °C. This process was repeated a few times until the fibers had completely turned white. After this, bleached fibers were washed with cold water. For the purification of fibers, bleached fibers were soaked in a mixture of 10 ml 65 % HNO_3 and 100 ml 80 % acetic acid and then placed in a preheated oil bath (120 °C) for 30 min. The acid hydrolysis was conducted by adding 64 wt% H_2SO_4 to the purified sample with a 10:1 ratio for 1 h at 45 °C under vigorous agitation. The reaction was quenched by diluting it with cold water. The diluted suspension was centrifuged at 12,000 rpm for 10 min, and this step was repeated several times until it turned into a turbid suspension. Final washing of the sample was performed by dialysis for 7 days. After dialysis, the suspension was sonicated (Digital ultrasonic cleaner, model ST-UB3300LDT) in an ice bath for 30 min. The resultant sample was freeze dried and stored in a drying cabinet.

Individualization of microfibrillated celluloses via APS oxidation

One liter of 1 M ammonium persulfate was prepared and added to 10 g OPEFB fibers, which were used as the starting biomass materials. The mixture was heated

at 60 °C for 16 h under constant mechanical stirring. Centrifugation of the treated suspension was carried out at 12,000 rpm for 10 min. The washing process was repeated four times until the pH of the suspension was close to 4. The sample was sonicated (Digital Ultrasonic Cleaner, model ST-UB3300LDT) in an ice bath 30 min prior to lyophilization. The lyophilized sample was stored in a drying cabinet.

Fourier transform infrared spectroscopy (FTIR)

Fourier transform infrared (FTIR) spectroscopy studies were performed using a PerkinElmer FTIR spectrophotometer (FT-IR spectrometer, PerkinElmer) to determine the functional groups of all the raw fibers, pre-acid hydrolysis-treated fibers, sulfuric acid-hydrolyzed nanocelluloses and APS-treated nanofibers. Effects of the treatments on the chemical compositions can be tracked from the IR spectra. Samples were ground and mixed well with KBr (1:100, w/w), then pressed into thin pellets prior to analysis. FTIR analysis was performed in the transmittance mode with a wavenumber range of 4000–400 cm^{-1} and a resolution of 4 cm^{-1} at an accumulation of 32 scans. The positions of the peaks were determined by the OriginPro software.

Field-emission scanning electron microscopy (FESEM)

Bleached fibers and freeze-dried samples were mounted on aluminum stubs using double-sided adhesive carbon tapes, and the samples were sputter-coated with platinum using an auto fine coater (Jeol JFC-1600). Morphological characteristics were observed using a FESEM (Jeol JSM-7600F), operated in high vacuum mode with a 5-kV accelerating voltage. Fiber diameters were analyzed using ImageJ software.

X-ray diffraction (XRD) analysis

The crystallinities of raw OPEFB, acid-hydrolyzed MFCs and APS-oxidized MFCs were evaluated by X-ray diffraction study. Impacts of the treatments on the crystallinity index values of the celluloses can be investigated from the X-ray diffractograms. The X-ray diffraction patterns of the specimens were obtained from an X-ray diffractometer (PANalytical Empyrean) operated at 40 kV and 40 mA with Ni-filtered CuKα radiation. X-ray diffractograms were recorded from 10° to 60° at a scan rate of 2 s/step with 0.02° step size.

Crystallinity index (CrI) values were calculated from diffraction intensity data via the empirical method using the following equation (Segal et al. 1959):

$$\mathrm{CrI}\,(\%) = \frac{I_{002} - I_{\mathrm{AM}}}{I_{002}} \times 100 \quad (1)$$

where I_{002} represents the maximum intensity of the 0 0 2 reflection peak and I_{AM} is the minimum value, which corresponds to the reflection intensity of the amorphous phase. The diffraction peak for plane 0 0 2 is located at a diffraction angle close to 26°, corresponding to the crystalline part, and the intensity scattered by the amorphous part is measured at the 2θ angle close to 15°.

Thermogravimetric analysis (TGA)

Thermal properties of the samples were analyzed by a thermogravimetric analyzer (TGA) (TGA 4000, PerkinElmer). Samples were placed in a crucible and heated under nitrogen atmosphere from 35 to 600 °C with the heating rate of 10 °C/min.

Optical transmittance

Bleached fiber and nanofiber suspensions were prepared and introduced into a quartz cuvette. The optical transmittance was measured between 300 and 800 nm using a Shimadzu UV-Vis spectrophotometer (UV-2600, Shimadzu). A cuvette filled with distilled water was used as blank.

Results and discussions

FTIR analysis

FTIR spectroscopy is an appropriate technique to monitor the variations in the chemical compositions of the samples in response to different treatments. As presented in Figs. 1 and 2, all the treated and untreated OPEFBs exhibited two major absorbance regions, which included the regions at high (2800–3500 cm^{-1}) as well as low wavenumbers (500–1700 cm^{-1}),

consistent with the previous studies (Ching et al. 2013; Fahma et al. 2010). Figure 1 displays the FTIR spectra of all the pretreated samples before digestion by sulfuric acid. Based on the spectra obtained, there were slight changes in the chemical compositions after the alkaline treatment and the bleaching process.

A dominant and broad absorption band located from 3500 to 3400 cm^{-1} and peak at approximately 2900 cm^{-1} were observed in the entire spectra, ascribed to the OH and CH stretching, respectively (Satyamurthy et al. 2011; Seng et al. 2014). A prominent peak at 1735 cm^{-1} could be observed in the spectra of raw OPEFB and fiber after Soxhlet extraction, but it totally vanished in the other spectra. The peak at 1735 cm^{-1} was associated with the presence of the acetyl and uronic ester groups of the hemicelluloses or to the ester linkage of the carboxylic groups of the ferulic and p-coumeric acids of lignin and/or hemicellulose (Sain and Panthapulakkal 2006). The disappearance of this peak substantiated that most of the hemicelluloses and lignin were removed effectively after NaOH and $NaClO_2$ treatments (Cherian et al. 2008).

However, the IR spectrum of APS-derived nanocelluloses, as shown in Fig. 2b, displayed a signal at 1735 cm^{-1}, indicating the presence of a C=O band, which was the most notable difference observed in respect to acid-hydrolyzed nanofibers. The APS-oxidized sample had peaks at 3400 cm^{-1} and 1735 cm^{-1}, demonstrating the presence of carboxylic acid groups (Leung et al. 2011). In addition, the peak

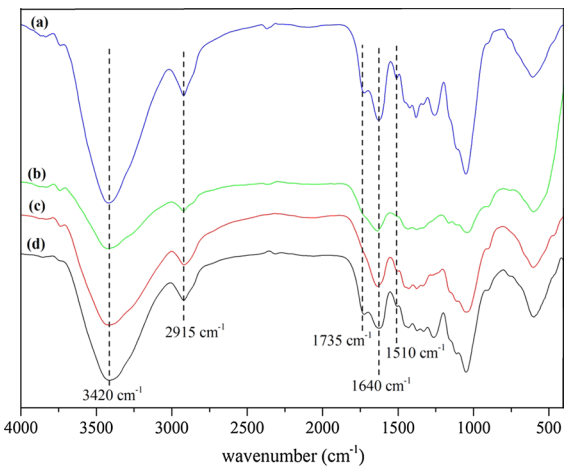

Fig. 1 FTIR spectra of **a** raw OPEFB, **b** bleached OPEFB, **c** alkaline-treated fibers and **d** OPEFB after Soxhlet extraction

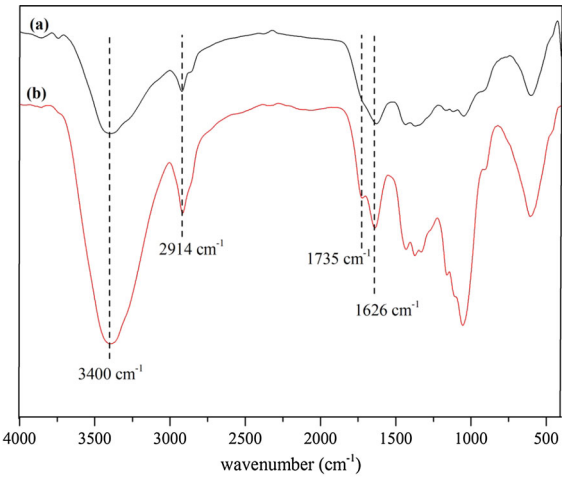

Fig. 2 FTIR spectra of **a** acid-hydrolyzed MFCs and **b** APS-treated MFCs

at approximately 1510 cm^{-1} was another significant signal for tracking the presence of the lignin as it represented the C=C stretching vibration in the aromatic ring of lignin (Chen et al. 2011a, b; Sun et al. 2000). This characteristic peak disappeared completely after the bleaching process, indicating that $NaClO_2$ had successfully dissolved the lignin components of OPEFB. The peak at approximately 1640 cm^{-1} observed in all the spectra corresponded to the H–O–H stretching vibration of the water molecules absorbed by the OPEFB fiber as OPEFB is hygroscopic in nature (Chen et al. 2011a, b).

Morphological investigation

Figure 3 depicts the FESEM micrographs of bleached fibers (Fig. 3a), acid-hydrolyzed MFCs (Fig. 3b) and APS-derived MFCs (Fig. 3c). The pristine OPEFB fiber is composed of microfibril bundles tangled with massive nonfibrous components, namely hemicelluloses and lignin (Fatah et al. 2014; Alemdar and Sain 2008; Johar et al. 2012). However, Fig. 3a shows individualized fibrils under FESEM observation, indicating the elimination of cementing materials after the bleaching process, which was in strong agreement with the spectroscopic results.

As mentioned in the procedure description, OPEFB fibers were treated by NaOH prior to bleaching using $NaClO_2$. NaOH treatment facilitated the dissolution of hemicelluloses and partial depolymerization of the

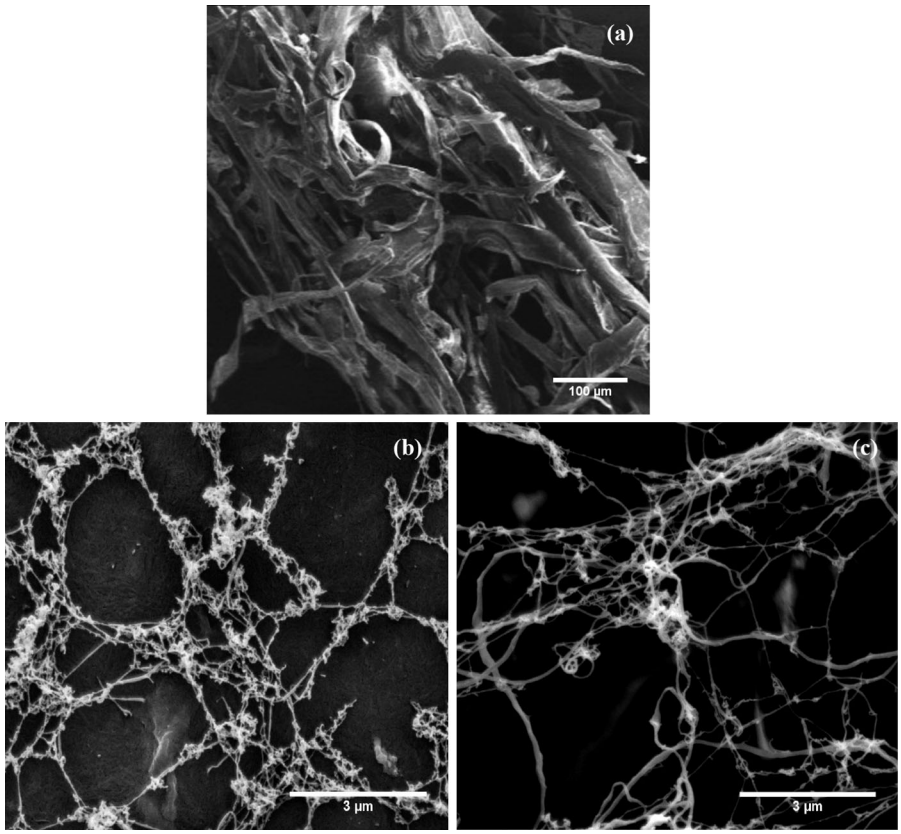

Fig. 3 FESEM micrographs of **a** bleached fibers, **b** sulfuric acid-hydrolyzed MFCs and **c** APS-derived MFCs

lignin and also induced the segregation of fiber bundles into elementary fibers. Meanwhile, the bleaching process helped to exclude most of the lignin present in OPEFB fibers effectively, contributing to further defibrillation and reduction of the fiber diameter. The bleaching agent containing chlorine was able to oxidize the lignin and stimulate the formation of hydroxyl carbonyl and carboxylic groups, which in turn facilitated the solubilization of lignin in an alkaline medium (Cherian et al. 2010). The bleached fibers were found to have an average mean of 14 µm.

The results revealed that the fiber diameter diminished to the nanometer scale after the acid hydrolysis reaction and APS treatment. Both sulfuric acid-hydrolyzed MFCs (Fig. 3b) and APS-derived MFCs (Fig. 3c) exhibited long and network-like fibrils, whereby the morphologies of both samples were similar to the morphologies of the MFCs obtained by Zimmermann et al. (2010). Aggregation of nanocelluloses can be observed in Fig. 3b, c, which is a common phenomenon reported by many previous studies (Kargarzadeh et al. 2012; Lu and Hsieh 2012; Rubentheren et al. 2015). Self-assembly of cellulose can be due to hydrogen bonding and depends on the species as well as separation method of the nanofibers (Hult et al. 2001). Nanofibers hydrolyzed an hour in sulfuric acid have diameters ranging from 8 to 26 nm, with the majority at approximately 16 nm. Meanwhile, 16-h APS-treated nanofibers have a mean diameter of 23 nm. Nevertheless, it was difficult to obtain an appropriate measurement of the length of both APS-oxidized and acid-hydrolyzed MFCs because of the difficulty in assigning the ends of the MFCs.

Fatah et al. (2014) also reported on the isolation of nanofibers from OPEFB by sulfuric acid hydrolysis but with the assistance of mechanical disintegration. They treated the bleached OPEFB with 30 % H_2SO_4 solution at 60 °C for 2 h with an acid-to-fiber ratio of 17.5:1 and successfully reduced the size of the fibers to

9 ± 1 μm, along with the shortened length of fibers. This revealed that the sizes of the resulting fibers after acid hydrolysis were strongly dependent on the acid concentration as well as the acid-to-fiber ratio. Furthermore, Dong et al. (1998) showed that 45 °C was more favorable for acid hydrolysis than higher temperatures such as 65 °C because higher temperatures can potentially lead to a dehydration reaction. For extraction of nanofibers by APS, Lam et al. (2013) prepared rod-shaped nanowhiskers from microcrystalline cellulose (Avicel PH102 microcrystalline cellulose, FMC Corp.) using APS oxidation, and the final fiber diameter was found to be approximately 5 nm. This indicated that the morphology and width of the nanocelluloses formed from APS treatment depend on the raw material used.

The nanofiber yield after acid hydrolysis and APS oxidation was determined by the weight difference. The yield percentage of the acid-hydrolyzed MFCs was approximately 25 %. Meanwhile, extraction via APS treatment was determined to produce about 40 % MFCs on a weight basis. This result showed that APS oxidation can effectively synthesize nanofibers in larger quantities with only one-step treatment.

Crystallinity studies

XRD studies were conducted to evaluate the crystalline behaviors of raw OPEFB and chemical-treated fibers. Celluloses are semicrystalline biopolymers known to comprise both crystalline and amorphous domains in their molecular structure. Crystalline regions are well-organized parts because of the hydrogen-bonding interactions and van der Waals forces between the molecules (Zhang and Lynd 2004; Nurfatimah et al. 2015). On the contrary, amorphous regions are disordered parts within the cellulose structures due to the absence of H-bonding (Jonoobi et al. 2011). The implications of different chemical treatments on the crystallinity index of the cellulose can be determined and compared from the XRD diffractogram profiles obtained. As shown in Fig. 4, diffractograms obtained for all the untreated and treated fibers exhibited similar patterns, which represent the typical semicrystalline materials with an amorphous broad hump and crystalline peak.

The crystallinity index for raw OPEFB, APS-treated MFCs and sulfuric acid-hydrolyzed MFCs was calculated based on Eq. (1) and found to be 75, 76

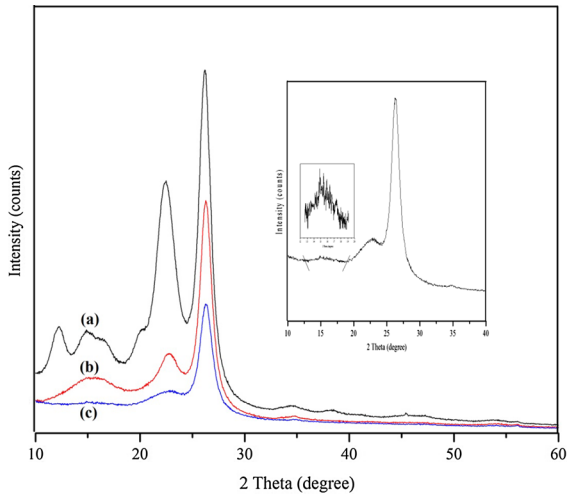

Fig. 4 XRD diffractograms of **a** acid-hydrolyzed MFCs, **b** APS-oxidized MFCs and **c** raw fibers. The inset displayed the XRD diffractogram of raw fibers with a more apparent amorphous hump (*inner*)

and 72 %, respectively. The crystallinity index of the MFC samples produced from OPEFB remained similar after the APS treatment. Leung et al. (2011) investigated APS oxidation on different cellulosic sources including flax, hemp, bacterial cellulose, commercial microcrystalline cellulose and fibrous cellulose powder (Whatman CF1). They reported that the crystallinity index for most of the nanofibers after the treatment was higher than for the parental counterparts except for nanofibers isolated from commercial microcrystalline cellulose and Whatman CF1. The crystallinity index of nanofibers prepared from commercial microcrystalline cellulose increased only slightly after APS oxidation and remained similar for Whatman CF1.

The crystallinity index of nanofibers after 60 min of hydrolysis was anticipated to be higher than for raw fibers because of the removal of a substantial part of the amorphous noncellulosic constituents including pectin, hemicelluloses and lignin, during the pretreatment steps (Chen et al. 2011a, b; Alemdar and Sain 2008; Li et al. 2009). Both alkalization and bleaching processes can effectively alter the crystallographic structure of fibers and eliminate the surface impurities, which are vital for the enhancement of the fiber-matrix interaction. This occurs because both of these treatment stages induce the exposure of the hydroxyl groups for the bonding reactions (Abraham et al. 2011).

After sulfuric acid hydrolysis, it was postulated to have a further increment in crystallinity as the hydronium ions could penetrate into the more accessible amorphous domains of cellulose, promoting the hydrolytic cleavage of glycosidic bonds and eventually liberating the elementary crystallites (Li et al. 2009). Moreover, higher crystallinity could be achieved during the self-assembly of nanocellulose as the realignment occurred in this natural phenomenon, enabling close packing and hydrogen bond formation (Li et al. 2009; Lu and Hsieh 2012). However, the crystallinity index of nanofibers after 60 min of hydrolysis was determined to decrease slightly, which was possibly the consequence of excessive exposure to concentrated sulfuric acid. According to Fahma et al. (2010), the crystallinity of fibers tended to decline slightly after 60 min of sulfuric acid hydrolysis as well. They reported that the crystallinity index of nanofibers prepared from OPEFB by 60 min of sulfuric acid hydrolysis was about 54 %, with the raw OPEFB being 55 %. Furthermore, alkaline treatment was also believed to be able to consume the crystalline cellulose while increasing the amount of amorphous cellulose, as shown in the XRD pattern of acid-hydrolyzed nanofibers (John and Anandjiwala 2008).

Cellulose can be generally classified into four different polymorphs: cellulose I, II, III and IV. It is worth noting that the cellulose forms can be recognized from the XRD patterns. In fact, no doublet will be observed in the main peak at 2θ at 26° for a typical cellulose I structure, which was demonstrated by pristine OPEFB. However, a doublet appeared in the major peak after chemical treatments, as shown in Fig. 4c, indicating the transformation of native cellulose from cellulose I to cellulose II (Lani et al. 2014). This conversion can be explained by the formation of a new Na-cellulose-I lattice through the alkaline pretreatment before the acid hydrolysis reaction. In this lattice structure, OH groups of the cellulose are replaced by ONa groups, expanding the molecule dimensions. Subsequent rinsing with water will remove the linked Na ions and lead to transformation into the most stable crystalline structure, which is cellulose II (John and Anandjiwala 2008).

Cellulose crystallinity is of prime importance as this is a key factor to determine the reinforcing capability and mechanical strength of cellulose to be utilized in composite applications. The highly crystalline fibers are expected to be more effective in providing higher reinforcement for composite materials owing to the increased stiffness and rigidity, achieving a higher Young's modulus (Cheng et al. 2007).

Thermostability analysis

Thermogravimetric analysis was used to investigate the thermal stability of the untreated and treated fibers. Determination of the thermal characteristics of the reinforcing materials is essential to evaluate the applicability of these materials in biocomposite applications at high temperatures. Both TG and dTG curves were plotted, as shown in Figs. 5 and 6, to track the thermal stability differences for all the samples. The dTG curves allowed for more precise assessment and comparison.

An initial weight loss was observed for all the samples upon heating to 100 °C, resulting from the vaporization of the loosely bound moisture on the surface of the materials (Fahma et al. 2010; Kargarzadeh et al. 2012; Yong et al. 2015b). According to Morán et al. (2007), another reason for this small weight loss was the degradation of the low molecular compounds remaining after various treatment stages. Raw OPEFB pyrolyzation was detected at different stages because it consists of various constituents, including hemicelluloses, lignin and cellulose. This observation was expected because cellulosic and noncellulosic components decompose at different

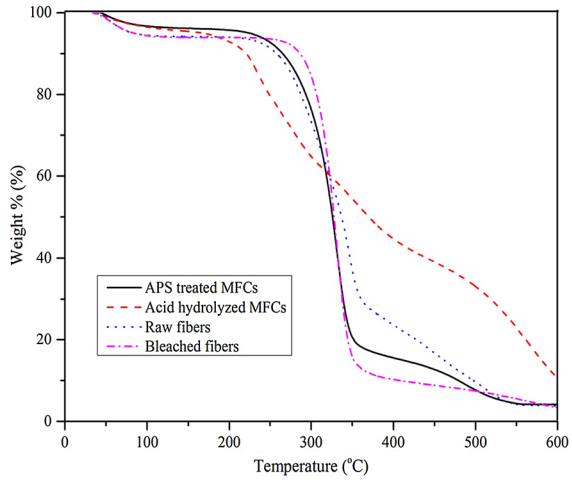

Fig. 5 TG curves of APS-treated MFCs, acid-hydrolyzed MFCs, raw fibers and bleached fibers

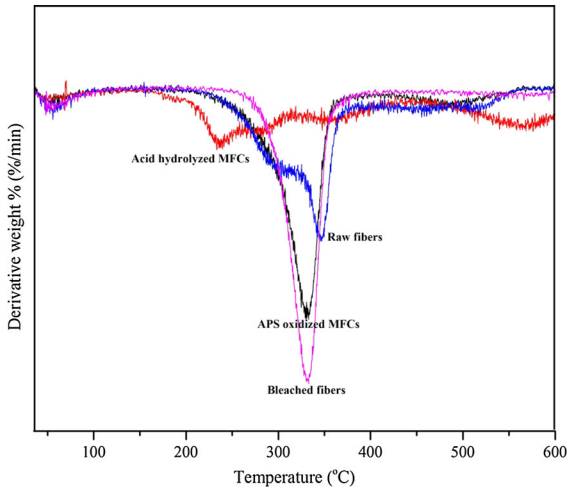

Fig. 6 dTG curves of APS-treated MFCs, acid-hydrolyzed MFCs, raw fibers and bleached fibers

temperatures (Morán et al. 2007; Yang et al. 2007). A low temperature shoulder was clearly observed in the dTG curve of raw OPEFB, which was ascribed to the degradation of hemicellulose (Morán et al. 2007). Hemicellulose decomposed at a lower temperature than lignin and cellulose, and this was attributed to the presence of acetyl groups in its structure. Meanwhile, there was another noticeable peak at around 350 °C corresponding to the pyrolysis of cellulose (Kargarzadeh et al. 2012).

The findings revealed that there were two decomposition stages for sulfuric acid-hydrolyzed nanofibers at approximately 235 and 350 °C, in accordance with the previous study reported by Mandal and Chakrabarty (2011) (Fig. 5). It was plausible to postulate that the early decomposition temperature is the consequence of the hydrolysis process, which results in a massive reduction of the molecular weight (Mohamad Haafiz et al. 2013). Furthermore, it was also believed that sulfuric acid hydrolysis not only removes the noncrystalline segment, but could also potentially dissolve some crystalline segments, making it more susceptible to degradation in response to rising temperature (Mandal and Chakrabarty 2011). Moreover, two different decomposition stages can also be explained by the presence of highly sulfated amorphous domains and unsulfated crystalline domains. The highly sulfated regions were more susceptible to degradation at lower temperature, whereas the higher temperature decomposition corresponded to the breakdown of unsulfated crystals (Kargarzadeh et al. 2012), while both bleached fibers and APS-derived MFCs showed a major peak at 330 °C, which represented the decomposition of cellulose.

Previous studies (Wang et al. 2007; Roman and Winter 2004; Kim et al. 2001) reported that a longer hydrolysis period induced the incorporation of more negatively charged sulfate groups to cellulose surfaces and led to a reduction in the thermostability of treated nanofibers. Sulfate groups replaced the OH groups of celluloses, leading to dehydration reactions. Cellulose degradations can be catalyzed because the activation energies of cellulose chain degradations were lowered by dehydration reactions (Roman and Winter 2004; Wang et al. 2007). In addition, a long hydrolysis time also cleaved celluloses into short chains, providing a large surface area and resulting in a low degree of polymerization that tended to degrade at low temperatures (Wang et al. 2007). The large surface area diminished the thermal stability of the cellulose because of the increased exposure to heat (Lu and Hsieh 2010).

The low thermal properties of acid-hydrolyzed nanofibers can be solved by neutralization with NaOH (Wang et al. 2007; Favier et al. 1995; Martínez-Sanz et al. 2011) or by conducting the hydrolysis using different acid species such as hydrochloric acid (HCl) to replace H_2SO_4 (Mohamad Haafiz et al. 2013). After neutralization with NaOH, no acid sulfate groups remained, and the thermal stability was shifted to a higher temperature, but the crystallinity was similar. Therefore, sulfate group contents play a significant role in determining the thermal properties of the materials (Kargarzadeh et al. 2012). In addition, the sulfated groups were recognized to be flame retardants. For this reason, the char fraction increased with an increasing amount of sulfated groups. As a result, the amount of char residue remaining after 600 °C was found to be higher for hydrolyzed fibers (Roman and Winter 2004).

Optical transmittance

UV-Vis spectroscopy was carried out to obtain information on the impacts of different treatments on the transparency of the MFC suspensions. The degree of transparency also reflects the size of the fibers. The transmittance is strongly dependent on the wavelength; it decreases with decreasing wavelength (Benhamou et al. 2014). Indeed, light will scatter

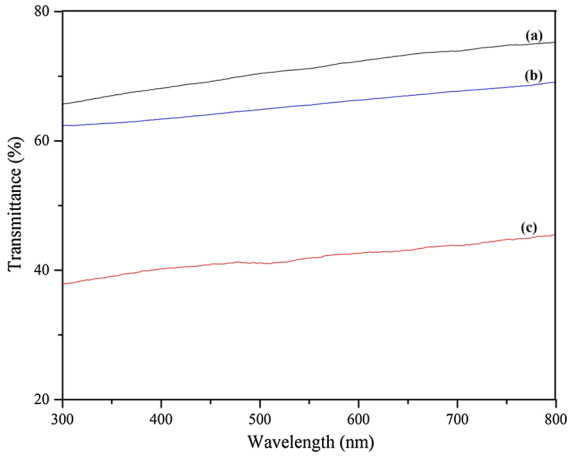

Fig. 7 UV-Vis transmittance spectra of **a** acid-hydrolyzed nanofiber suspensions, **b** APS-oxidized nanofiber suspensions and **c** bleached OPEFB

when it passes through a nanocellulose suspension containing randomly dispersed particles because the scattering occurs when there is a discontinuation in the refractive index, eventually causing a reduction in the transparency degree (Besbes et al. 2011). In addition, light will scatter more when the wavelength approaches the width of the dispersed particles (Saito et al. 2006). As observed from the UV-Vis spectra in Fig. 7, acid-hydrolyzed nanofibers were noted to have the highest optical transmittance followed by APS-oxidized nanofibers and bleached fibers. This indicated that the nanofibers generated by acid hydrolysis had smaller sizes than APS-derived nanofibers. These results were in accordance with the observations from FESEM.

Conclusion

MFCs were readily isolated from OPEFB by sulfuric acid hydrolysis and APS treatment without the assistance of mechanical disintegrations such as homogenization and microfluidization. The pronounced difference between these two methods was that the APS-derived MFCs were stabilized by carboxyl groups, while sulfuric acid-hydrolyzed MFCs were stabilized by sulfate half ester groups. MFCs prepared by APS oxidation were more thermally stable than those extracted by sulfuric acid hydrolysis because of the presence of the sulfate ester groups. In addition, 60 min of sulfuric acid hydrolysis was found to damage some of the crystalline segments, which eventually led to decreased in crystallinity. Furthermore, tedious and multiple pretreatment steps involved in the removal of noncellulosic components such as hemicelluloses, lignin and waxes were required prior to sulfuric acid hydrolysis. Hence, the time consumption to produce MFCs by sulfuric acid hydrolysis was longer than by APS treatment. Most importantly, the final yield of MFCs extracted by sulfuric acid hydrolysis was approximately 25 %, which was lower than the final productions of APS-derived MFCs ($\sim$40 % on a weight basis). Therefore, we can conclude that the simple and versatile APS oxidation is a better and more practicable method for large-scale production of MFCs.

Acknowledgments The authors would like to acknowledge the financial support of the High Impact Research MoE Grant UM.C/625/1/HIR/MoE/52 from the Ministry of Education of Malaysia, RU022B-2014, RP011A-13AET, RG031-15AET, PG036-2015A, FP053-2015A and FP030-2013A, which facilitated the success of this project.

References

Abraham E, Deepa B, Pothan LA, Jacob M, Thomas S, Cvelbar U, Anandjiwala R (2011) Extraction of nanocellulose fibrils from lignocellulosic fibres: a novel approach. Carbohydr Polym. doi:10.1016/j.carbpol.2011.06.034

Alemdar A, Sain M (2008) Isolation and characterization of nanofibers from agricultural residues–Wheat straw and soy hulls. Bioresour Technol 99(6):1664–1671

Ashiqur R, Ching YC, Yong KC, Nur A, Ashok KC, Chuah CH, Liou NS (2015) Surface modification of natural fiber using Bi_2O_3/TiO_2 composite for photocatalytic self-cleaning. BioResource 10(4):7405–7418. doi:10.15376/biores.10.4.7405-7418

Azizi Samir MAS, Alloin F, Dufresne A (2005) Review of recent research into cellulosic whiskers, their properties and their application in nanocomposite field. Biomacromolecules 6(2):612–626

Benhamou K, Dufresne A, Magnin A, Mortha G, Kaddami H (2014) Control of size and viscoelastic properties of nanofibrillated cellulose from palm tree by varying the TEMPO-mediated oxidation time. Carbohydr Polym 99:74–83

Besbes I, Vilar MR, Boufi S (2011) Nanofibrillated cellulose from alfa, eucalyptus and pine fibres: preparation, characteristics and reinforcing potential. Carbohydr Polym 86:1198–1206

Castro-Guerrero CF, Gray DG (2014) Chiral nematic phase formation by aqueous suspensions of cellulose nanocrystals prepared by oxidation with ammonium persulfate. Cellulose 21(4):2567–2577

Chen W, Yu H, Liu Y (2011a) Preparation of millimeter-long cellulose I nanofibers with diameters of 30–80 nm from

bamboo fibers. Carbohydr Polym. doi:10.1016/j.carbpol.2011.04.061

Chen W, Yu H, Liu Y, Chen P, Zhang M, Hai Y (2011b) Individualization of cellulose nanofibers from wood using high-intensity ultrasonication combined with chemical pretreatments. Carbohydr Polym. doi:10.1016/j.carbpol.2010.10.040

Cheng Q, Wang S, Rials TG, Lee S-H (2007) Physical and mechanical properties of polyvinyl alcohol and polypropylene composite materials reinforced with fibril aggregates isolated from regenerated cellulose fibers. Cellulose 14(6):593–602

Cherian BM, Pothan LA, Nguyen-Chung T, Gn Mennig, Kottaisamy M, Thomas S (2008) A novel method for the synthesis of cellulose nanofibril whiskers from banana fibers and characterization. J Agric Food Chem 56(14):5617–5627

Cherian BM, Leão AL, de Souza SF, Thomas S, Pothan LA, Kottaisamy M (2010) Isolation of nanocellulose from pineapple leaf fibres by steam explosion. Carbohydr Polym 81(3):720–725

Cherian BM, Leão AL, de Souza SF, Costa LMM, de Olyveira GM, Kottaisamy M, Nagarajan ER, Thomas S (2011) Cellulose nanocomposites with nanofibres isolated from pineapple leaf fibers for medical applications. Carbohydr Polym 86(4):1790–1798

Ching YC, Ng TS (2014) Effect of preparation conditions on cellulose from oil palm empty fruit bunch fiber. Bioresource 9(4):6373–6385

Ching YC, Goh KY, Luqman CA, Kalyani N (2013) Effect of nanosilica and titania on thermal stability of polypropylene/oil palm empty fruit fibre composite. J Biobased Mater Bioenergy 7:169–174

Ching YC, Ashiqur R, Yong KC, Nazatul LS, Cheng HC (2015) Preparation and characterization of polyvinyl alcohol-based composite reinforced with nanocellulose and nanosilica. BioResources 10(2):3364–3377

Coburn J, Gibson M, Bandalini PA, Laird C, Mao H-Q, Moroni L, Seliktar D, Elisseeff J (2011) Biomimetics of the extracellular matrix: an integrated three-dimensional fiber-hydrogel composite for cartilage tissue engineering. Smart Struct Syst 7(3):213

Dong XM, Revol J-F, Gray DG (1998) Effect of microcrystallite preparation conditions on the formation of colloid crystals of cellulose. Cellulose 5(1):19–32

El-Saied H, Basta AH, Hassanen ME, Korte H, Helal A (2012) Behaviour of rice-byproducts and optimizing the conditions for production of high performance natural fiber polymer composites. J Polym Environ 20(3):838–847

Ershad A, Yong KC, Ching YC, Chuah CH, Liou NS (2015) Effect of single and double stage chemically treated kenaf fibers on mechanical properties of polyvinyl alcohol film. BioResource 10(1):822–838

Fahma F, Iwamoto S, Hori N, Iwata T, Takemura A (2010) Isolation, preparation, and characterization of nanofibers from oil palm empty-fruit-bunch (OPEFB). Cellulose. doi:10.1007/s10570-010-9436-4

Fatah I, Khalil H, Hossain M, Aziz A, Davoudpour Y, Dungani R, Bhat A (2014) Exploration of a chemo-mechanical technique for the isolation of nanofibrillated cellulosic fiber from oil palm empty fruit bunch as a reinforcing agent in composites materials. Polymers. doi:10.3390/polym6102611

Favier V, Chanzy H, Cavaille J (1995) Polymer nanocomposites reinforced by cellulose whiskers. Macromolecules 28(18):6365–6367

Ferrer A, Filpponen I, Rodriguez A, Laine J, Rojas OJ (2012) Valorization of residual empty palm fruit bunch fibers (EPFBF) by microfluidization: production of nanofibrillated cellulose and EPFBF nanopaper. Bioresour Technol. doi:10.1016/j.biortech.2012.08.108

Hsu S-C, Don T-M, Chiu W-Y (2002) Free radical degradation of chitosan with potassium persulfate. Polym Degrad Stab 75(1):73–83

Huang Z-M, Zhang Y-Z, Kotaki M, Ramakrishna S (2003) A review on polymer nanofibers by electrospinning and their applications in nanocomposites. Compos Sci Technol 63(15):2223–2253

Hult E-L, Larsson P, Iversen T (2001) Cellulose fibril aggregation-an inherent property of kraft pulps. Polymer 42(8):3309–3314

Jackson JK, Letchford K, Wasserman BZ, Ye L, Hamad WY, Burt HM (2011) The use of nanocrystalline cellulose for the binding and controlled release of drugs. Int J Nanomed. doi:10.2147/IJN.S16749

Janardhnan S, Sain MM (2007) Isolation of cellulose microfibrils–an enzymatic approach. Bioresources 1(2):176–188

Johar N, Ahmad I, Dufresne A (2012) Extraction, preparation and characterization of cellulose fibres and nanocrystals from rice husk. Ind Crops Prod. doi:10.1016/j.indcrop.2011.12.016

John MJ, Anandjiwala RD (2008) Recent developments in chemical modification and characterization of natural fiber-reinforced composites. Polym Compos 29(2):187–207

Jonoobi M, Khazaeian A, Tahir PM, Azry SS, Oksman K (2011) Characteristics of cellulose nanofibers isolated from rubberwood and empty fruit bunches of oil palm using chemo-mechanical process. Cellulose. doi:10.1007/s10570-011-9546-7

Kargarzadeh H, Ahmad I, Abdullah I, Dufresne A, Zainudin SY, Sheltami RM (2012) Effects of hydrolysis conditions on the morphology, crystallinity, and thermal stability of cellulose nanocrystals extracted from kenaf bast fibers. Cellulose. doi:10.1007/s10570-012-9684-6

Kim D-Y, Nishiyama Y, Wada M, Kuga S (2001) High-yield carbonization of cellulose by sulfuric acid impregnation. Cellulose 8(1):29–33

Lam E, Leung ACW, Liu Y, Majid E, Hrapovic S, Male KB, Luong JHT (2013) Green strategy guided by Raman Spectroscopy for the synthesis of ammonium carboxylated nanocrystalline cellulose and the recovery of byproducts. ACS Sustain Chem Eng. doi:10.1021/sc3001367

Lani NS, Ngadi N, Johari A, Jusoh M (2014) Isolation, characterization, and application of nanocellulose from oil palm empty fruit bunch fiber as nanocomposites. J Nanomater. doi:10.1155/2014/702538

Leung AC, Hrapovic S, Lam E, Liu Y, Male KB, Mahmoud KA, Luong JH (2011) Characteristics and properties of carboxylated cellulose nanocrystals prepared from a novel one-step procedure. Small. doi:10.1002/smll.201001715

Li R, Fei J, Cai Y, Li Y, Feng J, Yao J (2009) Cellulose whiskers extracted from mulberry: a novel biomass production. Carbohydr Polym. doi:10.1016/j.carbpol.2008.09.034

Li J, Wei X, Wang Q, Chen J, Chang G, Kong L, Su J, Liu Y (2012) Homogeneous isolation of nanocellulose from sugarcane bagasse by high pressure homogenization. Carbohydr Polym. doi:10.1016/j.carbpol.2012.07.038

Lin N, Bruzzese C, Dufresne A (2012) TEMPO-oxidized nanocellulose participating as crosslinking aid for alginate-based sponges. ACS Appl Mater Interfaces 4(9):4948–4959

Lu P, Hsieh Y-L (2010) Preparation and properties of cellulose nanocrystals: rods, spheres, and network. Carbohydr Polym. doi:10.1016/j.carbpol.2010.04.073

Lu P, Hsieh Y-L (2012) Preparation and characterization of cellulose nanocrystals from rice straw. Carbohydr Polym. doi:10.1016/j.carbpol.2011.08.022

Mahmoud KA, Male KB, Hrapovic S, Luong JH (2009) Cellulose nanocrystal/gold nanoparticle composite as a matrix for enzyme immobilization. ACS Appl Mater Interfaces 1(7):1383–1386

Mandal A, Chakrabarty D (2011) Isolation of nanocellulose from waste sugarcane bagasse (SCB) and its characterization. Carbohydr Polym. doi:10.1016/j.carbpol.2011.06.030

Martínez-Sanz M, Lopez-Rubio A, Lagaron JM (2011) Optimization of the nanofabrication by acid hydrolysis of bacterial cellulose nanowhiskers. Carbohydr Polym 85(1):228–236

Mohamad Haafiz MK, Eichhorn SJ, Hassan A, Jawaid M (2013) Isolation and characterization of microcrystalline cellulose from oil palm biomass residue. Carbohydr Polym. doi:10.1016/j.carbpol.2013.01.035

Morán JI, Alvarez VA, Cyras VP, Vázquez A (2007) Extraction of cellulose and preparation of nanocellulose from sisal fibers. Cellulose. doi:10.1007/s10570-007-9145-9

Ng TS, Ching YC, Awanis N, Ishenny N, Rahman MR (2014) Effect of bleaching condition on thermal properties and UV-transmittance of PVA/cellulose biocomposites. Mater Res Innov 18:400–404

Nurfatimah B, Ching YC, Luqman CA, Chantara TR, Nor A (2014) Effect of methyl methacrylate grafted kenaf on mechanical properties of polyvinyl chloride/ethylene inyl acetate composites. Compos A 63:45–50

Nurfatimah B, Ching YC, Luqman CA, Chantara TR, Nor A (2015) Thermal and dynamic mechanical properties of grafted kenaf filled poly(vinyl chloride)/ethylene vinyl acetate composites. Mater Des 65:204–211

Qua E, Hornsby P, Sharma H, Lyons G (2011) Preparation and characterisation of cellulose nanofibres. J Mater Sci 46(18):6029–6045

Roman M, Winter WT (2004) Effect of sulfate groups from sulfuric acid hydrolysis on the thermal degradation behavior of bacterial cellulose. Biomacromolecules 5(5):1671–1677

Rubentheren V, Thomas AW, Ching YC, Praveena N (2015) Physical and chemical reinforcement of chitosan film using nanocrystalline cellulose and tannic acid. Cellulose. doi:10.1007/s10570-015-0650-y

Sain M, Panthapulakkal S (2006) Bioprocess preparation of wheat straw fibers and their characterization. Ind Crops Prod 23(1):1–8

Saito T, Nishiyama Y, Putaux J-L, Vignon M, Isogai A (2006) Homogenous suspensions of individualized microfibrils from TEMPO-catalyzed oxidation of native cellulose. ACS Biomacromolecules 7(6):1667–1691

Satyamurthy P, Jain P, Balasubramanya RH, Vigneshwaran N (2011) Preparation and characterization of cellulose nanowhiskers from cotton fibres by controlled microbial hydrolysis. Carbohydr Polym 83(1):122–129

Segal L, Creely J, Martin A, Conrad C (1959) An empirical method for estimating the degree of crystallinity of native cellulose using the X-ray diffractometer. Text Res J 29(10):786–794

Sehaqui H, Allais M, Zhou Q, Berglund LA (2011) Wood cellulose biocomposites with fibrous structures at micro-and nanoscale. Compos Sci Technol 71(3):382–387

Seng KC, Ealid M, Ching YC, Haniff M, Khalid K, Beg MTH (2014) Preparation and characterization on polyvinyl alcohol/oil palm empty fruit bunch fiber composite. Mater Res Innov 18:364–367

Sun R, Tomkinson J, Wang Y, Xiao B (2000) Physico-chemical and structural characterization of hemicelluloses from wheat straw by alkaline peroxide extraction. Polymer 41(7):2647–2656

Tan BK, Ching YC, Gan SN, Ramesh S, Rahmmah RV (2014) Water absorption properties of kenaf fibre—PVA composites. Mater Res Innov 18:144–146

Tan BK, Ching YC, Gan SN, Ramesh S, Shaifulazuar R (2015) Biodegradable mulches based on poly(vinyl alcohol), kenaf fiber, and urea. Bioresources 10(3):5532–5543

Tanaka R, Saito T, Isogai A (2012) Cellulose nanofibrils prepared from softwood cellulose by TEMPO/NaClO/NaClO(2) systems in water at pH 4.8 or 6.8. Int J Biol. doi:10.1016/j.ijbiomac.2012.05.016

Wang N, Ding E, Cheng R (2007) Thermal degradation behaviors of spherical cellulose nanocrystals with sulfate groups. Polymer 48(12):3486–3493

Yang H, Yan R, Chen H, Lee DH, Zheng C (2007) Characteristics of hemicellulose, cellulose and lignin pyrolysis. Fuel 86(12):1781–1788

Yong KC, Ching YC, Mohamad A, Lim ZK, Chong KE (2015a) Mechanical and thermal properties of chemical treated oil palm empty fruit bunches fiber reinforced polyvinyl alcohol composite. J Biobased Mater Bioenergy 9:231–235

Yong KC, Ching YC, Cheng HC, Liou NS (2015b) Effect of fiber orientation on mechanical properties of kenaf-reinforced polymer composite. BioResources 10(2):2597–2608

Zhang YHP, Lynd LR (2004) Toward an aggregated understanding of enzymatic hydrolysis of cellulose: noncomplexed cellulase systems. Biotechnol Bioeng 88(7):797–824

Zhao J, Zhang W, Zhang X, Zhang X, Lu C, Deng Y (2013) Extraction of cellulose nanofibrils from dry softwood pulp using high shear homogenization. Carbohydr Polym 97(2):695–702

Zimmermann T, Bordeanu N, Strub E (2010) Properties of nanofibrillated cellulose from different raw materials and its reinforcement potential. Carbohydr Polym 79:1086–1093